AL15 - Simulation Optimization and Industrial Test of Fume Ductwork on Aluminum Reduction Cell

Yanfang Zhang[1], Dengpeng Chai[2] Yueyong Wang[3], Li Han[4], Qiaoyun Liu[5] and Yanhui Liu[6]
1. Professor
2. Professor
3. Senior Engineer
4. Engineer
5. Engineer
6. Engineer
Zhengzhou Non-ferrous Metals Research Institute Co.Ltd of CHALCO, Zhengzhou, China
Corresponding author: yanfzh@163.com.

Abstract

In a 400 kA smelter, there are some problems of the fume ductwork on the cells, such as serious alumina accumulation in the fume collecting duct, and large difference of fume volume collected between the duct end and the tap end. Even the fume escaped from the pot hood, which leads to random emission of the fumes to the potroom. In this paper, the existing structure of the fume ductwork of the reduction cells is studied by the simulation. The effects of the key factors are studied, and the design of an appropriate structure of the fume ductwork is optimized. The simulation results are verified by the industrial test on reduction cells. Test results show that the optimized fume ductwork exhausts fumes balanced between the duct end and the tap end, avoiding the fume escape from the pot hood of the tap end, and reduces the dust accumulation in the duct and the consumption of aluminum fluoride per ton of aluminum.

Keywords: Simulation optimization, fume ductwork, aluminum reduction cells.

1. Introduction

In a 400 kA smelter, there were some problems of the fume ductwork on the cells, such as a serious alumina accumulation in the fume collecting duct (shown in Figure 3), and large difference of fume volume collected between the duct end and the tap end. Even the fume escaped from the pot hood, which leads to the unorganized emission of the fume. In order solve these problems, the structure of the fume ductwork was improved, but the effect is not obvious. The original fume ductwork is shown in Figure 1, the improved and existing fume ductwork are shown in picture 2. Therefore, we need to re-simulate and optimize the design of the fume ductwork to reduce alumina accumulation and to improve the effect of the collected fume.

2. Simulation and Optimization of the Design of the Fume Ductwork

2.1. Modeling

2.1.1. Physical Model

According to the physical structure of the original design and existing design of the fume ductwork in the smelter, two physical models are established according to the design drawings. The original design is shown in Figure 1. The original design of the duct is divided into upper and lower parts. From the center of a cell to the tap end, the fume is collected from the round holes of the same size through the upper part. From the center of the cell to the duct end, the fume is

collected from the round holes of the same size through the lower part. All round, holes are evenly distributed in the same height of duct. The fume collecting duct has a semicircular bottom.
Figure 2 shows the new design of fume collecting duct with improvements based on the original design. The outlet of the upper duct is closed, as shown in Figure 4. The partition between upper and lower parts is opened, and all the fume goes through lower duct. The round holes from the center of the cell to the duct end are changed to square holes, and six discharge holes are added at the bottom of the duct pipe.

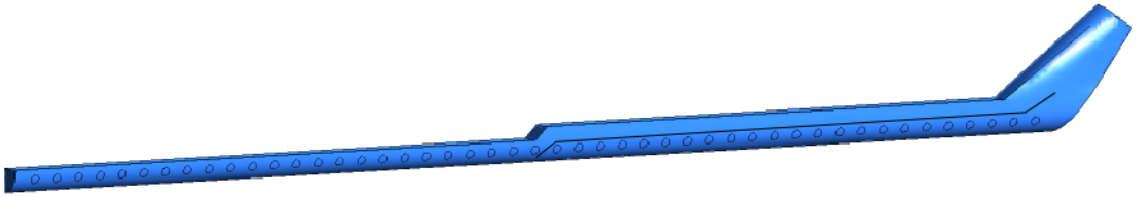

Figure 1. The original fume ductwork.

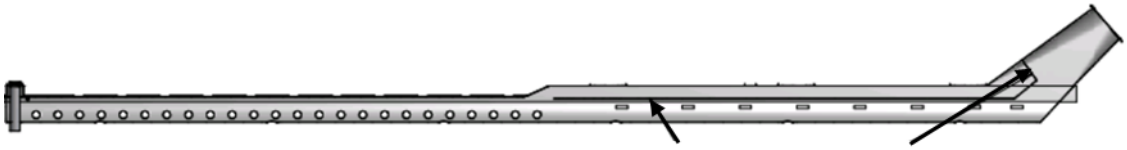

Figure 2. The new fume ductwork.

Figure 3. Accumulation of alumina in the duct.

Figure 4. The outlet of the upper duct is closed.

2.1.2. Governing Equations

As mentioned above, the dust accumulation in the duct is mainly caused by the insufficient discharge capability of the fume duct, which has few or no discharge holes or they are in unreasonable locations, and the difference in fume collection volume between tap end and duct end. The difference in fume collection volume between tap end and duct end is caused by the uneven fume collection between the two ends, and is not related to the temperature gradient. Therefore, the influence of temperature gradient is not considered in the simplified modeling, and the Fume Phase Turbulence Model is used in the simulation. The continuity and momentum governing equations are shown below.

Mass Conservation Equation
The equation for conservation of mass, or continuity equation, can be written as follows:

$$\nabla \cdot \rho\vec{v} = 0 \qquad (1)$$

Equation (1) is the general form of the mass conservation equation and is valid for incompressible as well as compressible flows.

Momentum Conservation Equations
Conservation of momentum in an inertial (non-accelerating) reference frame is described by

$$\nabla \cdot (\rho\vec{v}\vec{v}) = -\nabla p \qquad (2)$$

where p is static pressure.

Transport Equations for the Standard k-ε Model
The turbulence kinetic energy, k and its rate of dissipation, ε, are obtained from the following transport equations:

$$\frac{\partial}{\partial x_i}(\rho k u_i) = \frac{\partial}{\partial x_j}\left[\left(\mu + \frac{\mu_t}{\sigma_k}\right)\frac{\partial k}{\partial x_i}\right] + G_k - \rho\varepsilon \qquad (3)$$

and

$$\frac{\partial}{\partial x_i}(\rho\varepsilon u_i) = \frac{\partial}{\partial x_j}\left[\left(\mu + \frac{\mu_t}{\sigma_\varepsilon}\right)\frac{\partial \varepsilon}{\partial x_i}\right] + C_{1\varepsilon}\frac{\varepsilon}{k}(G_k + C_{3\varepsilon}G_b) - C_{2\varepsilon}\rho\frac{\varepsilon^2}{k} \qquad (4)$$

In these equations, G_k represents the generation of turbulence kinetic energy due to the mean velocity gradients, calculated as described in Modeling Turbulent Production in the k-ε Models. $C_{1\varepsilon}$, $C_{2\varepsilon}$ and $C_{3\varepsilon}$ are constants. σ_k and σ_ε are the turbulent Prandtl numbers for k and ε respectively.

The turbulent (or eddy) viscosity, μ_τ, is computed by combining k and ε as follows:

$$\mu_\tau = \rho C_\mu \frac{k^2}{\varepsilon} \qquad (5)$$

where C_μ is a constant.

2.2. Simulation Results of the Original and Existing Fume Ductwork

The original design and the existing design of the fume ductworks of the cells are simulated. As the simulation results show, the original duct is divided into two layers. One layer corresponds to the fume collecting holes of half-cell, so there are two trends in the curve of the mass flow rate of the collected fume by fume holes. The two largest fume mass flow rates lie in the cell center and duct end, and the fume mass flowrate gradually decreases towards the tap end, as shown in Figure 5. The negative pressure distribution at the outlet of the duct required for its fume resistance is shown in Figure 6. The fume collected mass flow rate of each collecting hole of the existing flume is shown in Figure 7, which decreases gradually from the duct end to the tap end, and the fume mass flow rate of the holes at half-cell near the tap end is too low, and the fume collection is very much uneven. Negative pressure distribution at the outlet of the duct required for its fume resistance as shown in Figure 7, with the average value is -463.4 Pa. The simulation results show that the effect of the existing ductwork still does not support a balanced fume collection after the ductwork being modified.

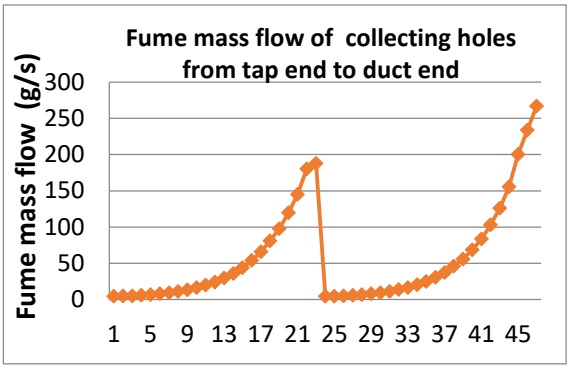

Figure 5. The original fume ductworks.

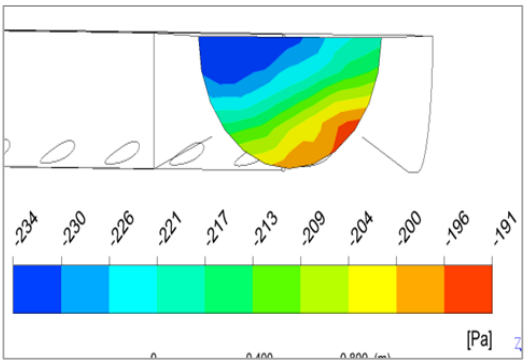

Figure 6 Pressure distribution of outlet.

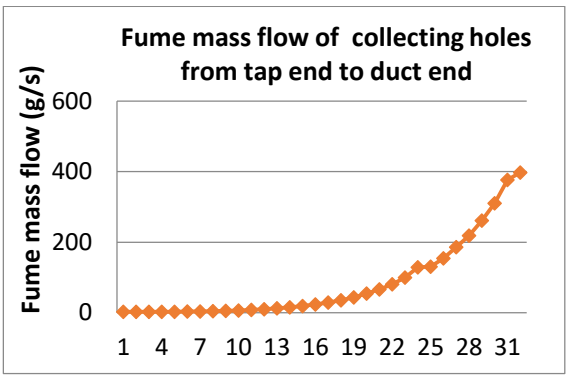

Figure 7. The existing fume ductworks.

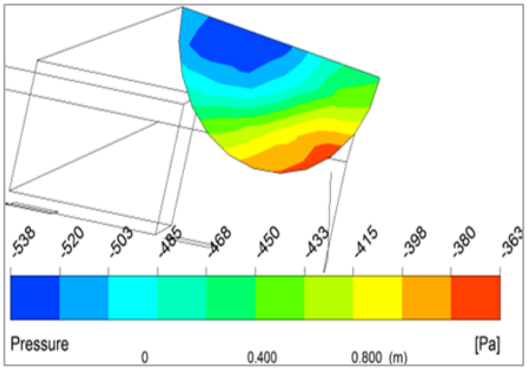

Figure 8. Pressure distribution of outlet.

2.3. Process and Result of Simulation Optimization

The simulation results of the existing ductwork shows: 1) due to the unreasonable size distribution of the fume collecting holes from the duct end to the tap end, the negative pressure of the fume collecting is released too much near the duct end , the negative pressure of each collecting hole near the tap end is insufficient, and the fume flow rate of the holes is gradually reduced, resulting in the fume collection volume different between both ends is too high; 2)With the speed of the collected fume decreasing in the duct, the alumina powder flying with the fume fall on the bottom of the duct and accumulates there. There is no discharge hole at the bottom of the arc-shaped duct or their size are not enough to drive out the alumina powder. The alumina be accumulated with time increasing, the smaller effective pipe space of the duct for fume collection will be, and the negative pressure required for fume collection will be increased.

Therefore, our optimization objectives and measures are as follows:

1) Aim to discharge alumina powder easily and decrease the accumulation, the discharge holes need to be arranged and sized reasonably, and the duct needs an inverted triangle section with the slope greater than the angle of repose of the alumina. Meanwhile, the uniformity of the fume collection of the discharge holes should also be ensured from the duct end to the tap end.
2) Aim to collect fume and heat uniformly from duct end to tap end - the sizes and positions of every fume hole need to be simulated and designed optimally, so to ensure the fume collection uniformity of the whole duct by the fume collecting ability of the discharge holes.
3) Reduce air resistance, to reduce the pressure loss and also the outlet pressure by optimizing the overall structure of the duct for the reduction of air resistance.

The measures taken are:
According to the above principles and the space constraints in the cell, minimum modification achieved better effect. The basic structure of the fume ductwork is designed as shown in Figure 9. The design firstly, eliminates the partition between the upper part and the lower part of the duct, secondly, the lower part of the duct has an inverted triangle section and the slope greater than the angle of repose of the alumina, replacing the original duct which had an arc-shaped bottom. Thirdly, many circular fume collecting holes with increasing diameter are placed on the upper part of both sides of the duct, and square discharge holes are evenly arranged at the duct bottom. Then each part is simulated and optimized to acquire an ideal design of the whole fume ductwork.

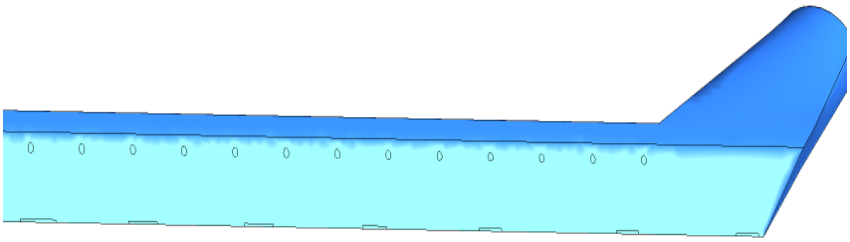

Figure 9. A foundation structure of the fume ductwork.

2.3.1 Homogenization of Fume Collection

Changing the area of each fume collecting hole and discharging hole ensures uniform volume of fume collection at each position of the cell. After a lot of optimization work, as shown in Table 1, Figure 10 and Figure 11, from scheme 1-1 to scheme1- 15, the simulation results show:

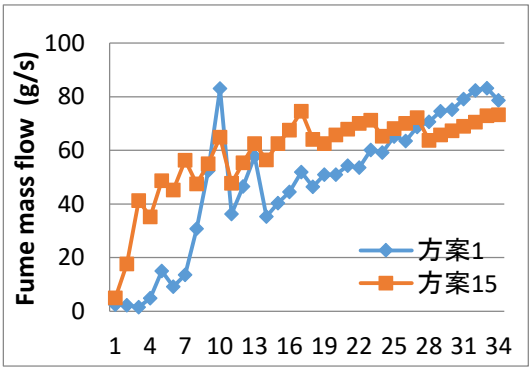

Figure 10. Fume mass flow of collecting holes from tap end to duct end.

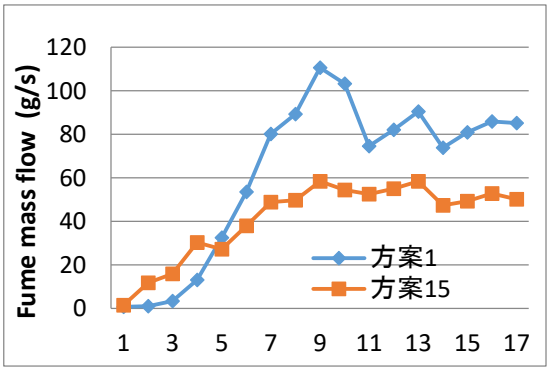

Figure 11 Fume mass flow of discharge holes from tap end to duct end.

1) If the air holes near the duct end are too large, the negative pressure of the fume collecting will be dissipated too fast, and the negative pressure of the collecting holes towards the tap end will be insufficient, so that the suction flow rate of these holes will be too small. Therefore, the diameter of each collecting hole from the duct end to the tap end should be gradually increased to improve the uniformity. However, if the hole diameter near duct end is decreased too much to improve the uniformity, the overall negative pressure requirement will be too high, as shown in Table 1. For more uniformity, more negative pressure is needed, even the average negative pressure is larger than in the current design (the existing fume ductwork). Considering the uniformity and negative pressure overall, 1-15 is selected as the uniformity foundation scheme for further optimization.
2) If a collecting hole is too small, being in the hole diameter gradient, the flow rate will be small. The streamline diagram shows that the fume cannot reach the outlet, as shown on

the left of Figure 12. The right side of Figure 12 shows the streamline of each hole optimized according to the simulation.

3) If the discharge hole near tap end is large and the pressure of these holes is small, increasing the size of the discharge hole cannot increase the flow rate, and will affect the flow rate of the collecting holes nearby, even backflow occurs, and the fume will get out of the round collecting holes above. So, keeping the area unchanged, the discharge hole should be lengthened along the longitudinal direction of the cell as much as possible to increase the discharge capacity without affecting the fume collection capacity. In all the simulation schemes, the scheme 1-15 is the best scheme.

Figure 12. Streamline diagram of collecting holes.

Table 1. Negative pressure comparison of optimization results of each scheme.

	Existing	Scheme 1-1	Scheme 1-5	Scheme 1-13	Scheme 1-15
Pmax (Pa)	-537.7	-445.7	-624.4	-547.6	-526.5
Pave (Pa)	-463.4	-408	-587.8	-512.2	-489

2.3.2 Increasing the Duct Height

Based on the scheme 1-15, under the condition of ensuring the balance, the duct height is increased, and the diameter of the collecting holes are all enlarged to reduce fume resistance of the duct. However, due to the space limitation, the duct can be increased by up to 100 mm. Simulation results are shown in Figure 13 and Table 2, the negative pressure of scheme 2-8 is reduced to - 380 Pa with better fume collected uniformity.

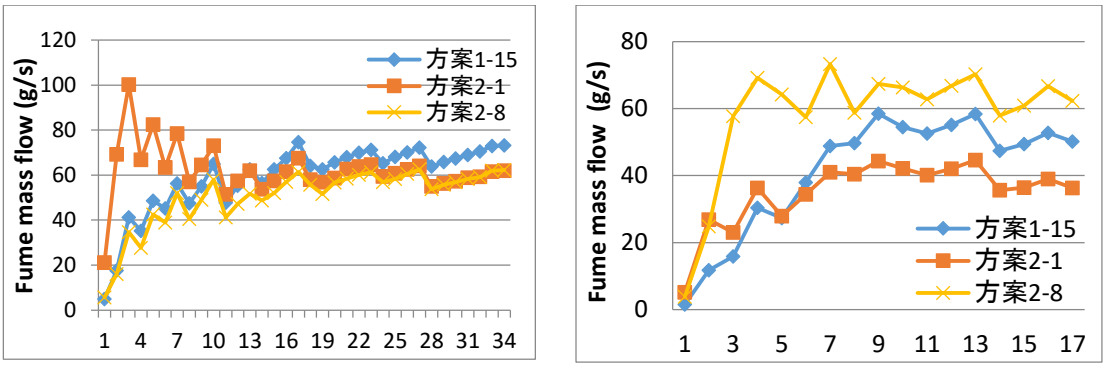

Figure 13. Fume mass flow of collecting holes and discharge holes from tap end to duct end.

Table 2. Negative pressure comparison of optimization results of each scheme.

	Existing	Scheme1-15(+0)	Scheme2-1(+50mm)	Scheme 2-8(+100mm)
Pmax (Pa)	-537.7	-526.5	-448.7	-410.2
Pave (Pa)	-463.4	-489.0	-411.7	-380.3

2.3.3 Optimization of Anti Blocking

After optimizing the fume collection equilibrium, the discharge capacity of the square hole at the bottom of the fume pipe should be considered. Under the condition that the area of the discharge hole remains unchanged, the height of the discharge hole is reduced and the length is increased, as shown in Figure 14. The aim is to increase the proportion of discharge parts of the pipe and then increase the discharge capacity without affecting the fume collection capacity. At the same time, a leakage hole is located at the intersection of horizontal duct and inclined duct to ensure that the alumina powder can be discharged in time due to the decrease of fume velocity because of the change of fume direction at this position.

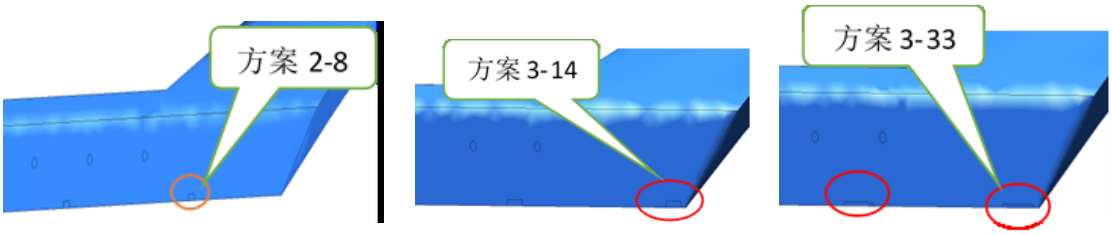

Figure 14. Position of discharge hole of each scheme.

Table 3. Size of discharge hole of each scheme.

Location	Scheme2-8	Scheme3-14	Scheme3-23	Scheme3-33
10	95×60	170×30	300×20	335×15
12	66×49	146×30	223×20	270×15
14	50×48	110×30	170×20	230×15
17	50×48	110×30	170×20	210×15

It can be seen from Figure 15 and Table 4 that under the condition of ensuring the fume collection equilibrium, the discharge hole of scheme 3-33 becomes longer and narrower, which increases the discharge capacity of the duct.

Table 4. Negative pressure comparison of optimization results of each scheme.

	Scheme2-8	Scheme3-14	Scheme3-23	Scheme3-33
Pmax (Pa)	-410.2	-399.3	-391.8	-395
Pave (Pa)	-380.3	-370.5	-362.1	-360.3

2.3.4 Optimization of Position Height of Fume Collecting Hole

This is a trial to adjust the position height of fume collecting holes. Scheme3-34 moves up 80 mm base on scheme 3-33. scheme 3-35 is that the left half holes move up 80 mm, the right half holes moves up 130 mm base on scheme 3-33, and scheme 3-36 moves up 100 mm on scheme 3-33 the same. The calculation results are shown in Table 4. It can be seen that scheme 3-34 is suitable.

Table 5. Negative pressure comparison of optimization results of each scheme.

	Scheme3-33	Scheme3-36	Scheme3-35	Scheme3-34
Pmax (Pa)	-395	-372.8	-372.5	-365
Pave (Pa)	-360.3	-352	-350.6	-350.1

2.3.5 Selection of the Scheme

Scheme 3-34 is slightly better optimized than the obtained scheme 4-7. Its structure, fume collection equilibrium and negative pressure results are shown in Figure 15, Figure 16 and in Table 5.

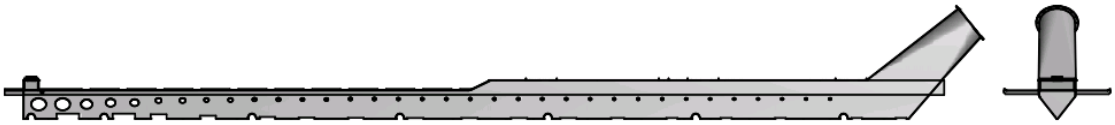

Figure 15. Structure of fume ductwork.

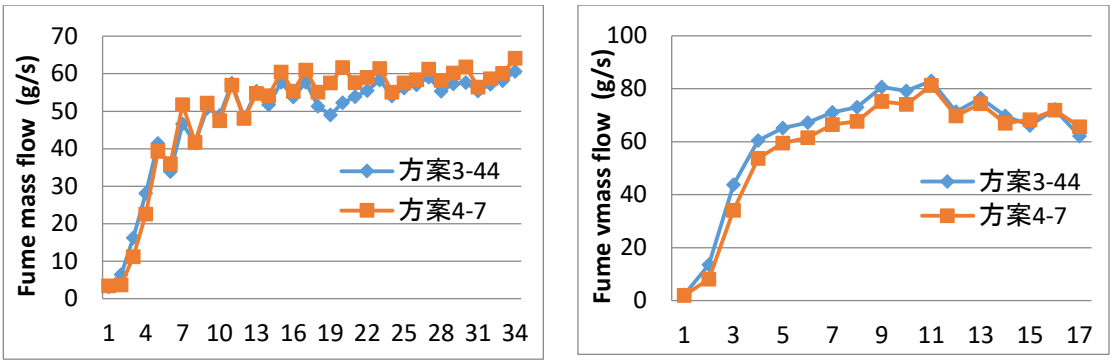

Figure 16. Fume mass flow rate of collecting holes and discharge holes from tap end to duct end.

Table 6. Negative pressure comparison of optimization results of each scheme.

Scheme	3-34	4-7
Pmax (Pa)	-365	-368.5
Pave (Pa)	-350	-347.5

2.3.6 Conclusion of Simulation and Optimization

Compared with the design before optimization, the negative pressure Pmax of the optimized results is reduced from 538 Pa to 368 Pa, and the average pressure Pave is reduced from 463 Pa to 347 Pa. The flow balance is also greatly improved, and the comparison is shown in Figure 17.

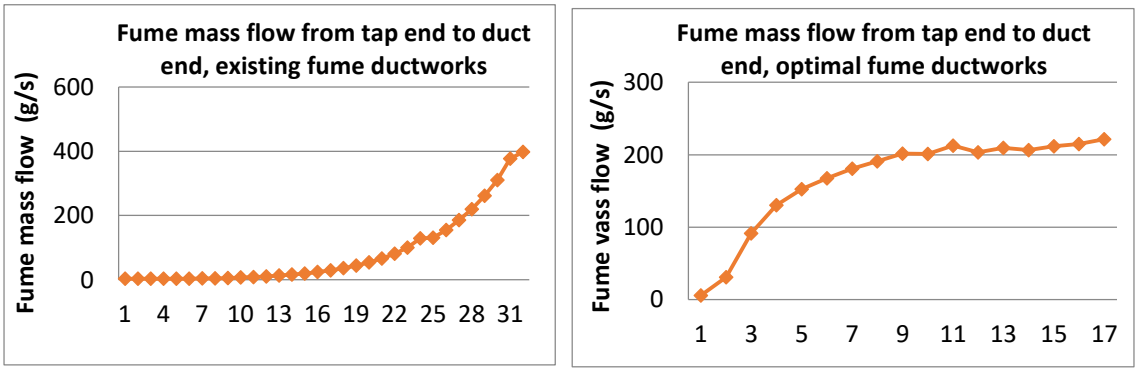

Figure 17. Comparison of results before and after optimization.

3. Industrial Test Results

Since 2016, the optimized design has been tested on a 400 kA cell. One month after the start-up of the test cell, due to the obviously positive effect, the optimized design has been approved for large scale implementation in the 300 kA and 400 kA cells. More than 100 cells have been modified. Both, for the smelter users' experience and the test data, the positive effect is significant.

3.1. Comparison of Fume Collection Equilibrium

It can be seen from the data that the equilibrium of fume collection in test cell 2250# is obviously better than that in comparison cell 2251#.

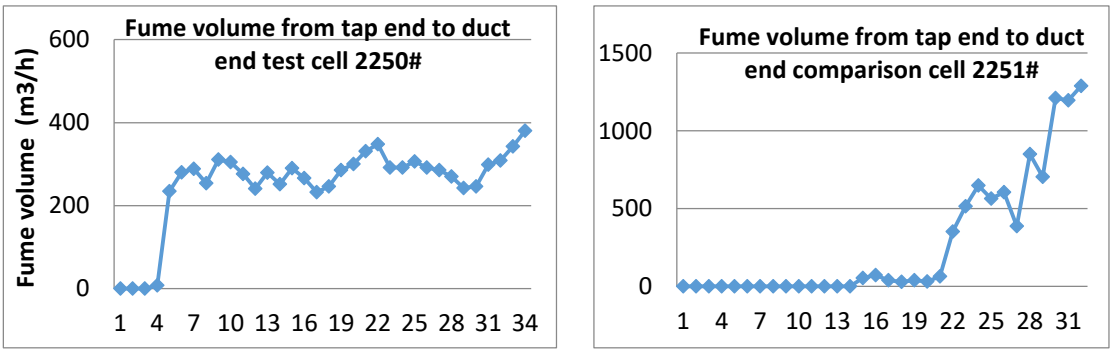

Figure 18. Test results of fume volume flow rate between test cell and comparison cell.

3.2. Comparison of Fume Flow in the Ductwork of Cells

The position from near fan to the far end, fume volume exhaust flowrate of six cells was tested; the cell positions are No.0, 1, 2, 7, 8, and 9. Magenta is unmodified cell, blue is redesigned cell. It can be seen that the fume volume exhaust rates are significantly greater in the redesigned cells, undoubtedly because the fume resistance of the duct on redesigned cells is reduced.

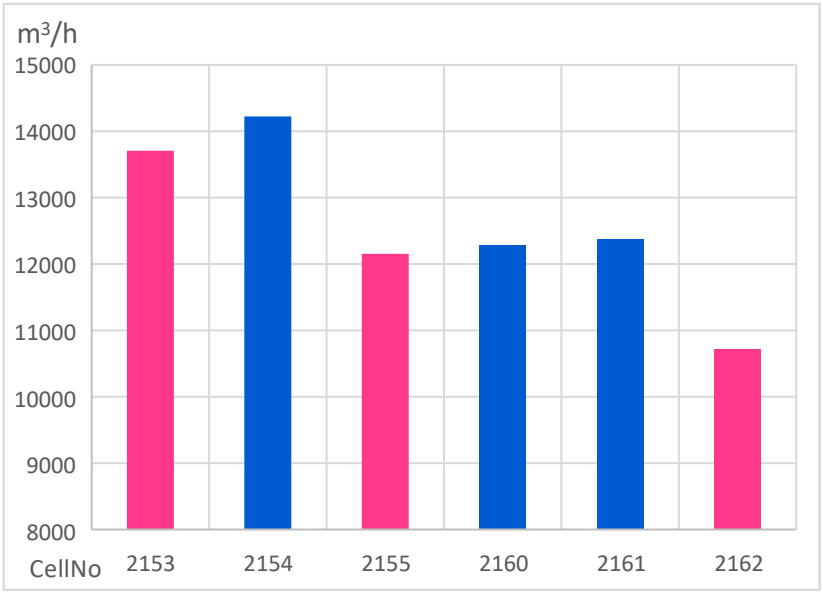

Figure 19. Fume exhaust volume flowrates of test cells and their neighboring unmodified cells.

3.3. Comparison of Fluoride Consumption

Since September 2017, the fluoride consumption of each cell has been statistically compared. The consumption of fluorine salt per ton of aluminum decreased by 2.4 kg as shown in Table 6. It also shows that the amount of alumina powder taken away is also reduced, and it can be seen that the alumina powder is constantly flowing from the discharge holes.

Table 7. Comparison of fluoride consumption.

Fluoride consumption	**Sept. 2017 – March 2018**	**April 2018 – October 2018**	**Sept. 2017 – October 2018**
49 original cells（kg/t Al）	23.4	26.8	25.1
61 test cells（kg/t Al）	20.9	24.6	22.7
Difference（kg/t Al）	2.5	2.2	2.4

4. Conclusions

Through the simulation and optimization research on the fume collecting duct of aluminium reduction cells, the industrial test verification and application on more than 100 electrolytic cells, the simulation data, operation test data and user experience, all show that the positive effect of the duct modification is remarkable. Balanced fume collection of the cell is achieved, the seriously uneven exhaust fume collection between tap end and duct end of the original design is improved, the random emissions into the potroom are reduced and the environmental pollution is reduced. Equally, the alumina accumulation in the duct is reduced to ensure the fume collection efficiency in continuously during cell operation. The fume resistance of the duct is reduced and the fan energy consumption is reduced. The consumption of aluminum fluoride per ton of aluminum is also reduced by 2.4 kg.